Supplementary Information (SI) for Materials Advances.

Oxidation Behavior of Iron and Binder-Mixed Iron: Insights from TGA-DSC and In-Situ XRD Analysis for Field Emission Application

Supriya E. More [a,b], Suyog A. Raut [a,d], S. Premkumar [a,c], Somnath R. Bhopale [a,f], Davy Deduytsche [e], Sudha V. Bhoraskar [a], Mahendra A. More [a], Damien Thiry [d], Christophe Detavernier [e], Nathalie De Geyter [b], Vikas L. Mathe [a*], Rino Morent [b]*

[a] Department of Physics, Savitribai Phule Pune University, Ganeshkhind, Pune 411007, Maharashtra, India.

[b] Research Unit Plasma Technology (RUPT), Department of Applied Physics, Ghent University, Ghent, 9000 Belgium.

[c] Armament Research and Development Establishment (ARDE), Pune 411021, Maharashtra, India.

[d] Chimie des Interactions Plasma-Surface (ChIPS), Université de Mons, Mons, 7000 Belgium.

[e] Department of Solid States Science, Krijgslaan, Ghent University, Ghent, 9000 Belgium.

[f] School of Physics, IISER Thiruvananthapuram, Vithura, Thiruvananthapuram, Kerala 695551, India

Figure S1 shows in-situ X-ray diffraction (XRD) patterns of the M-Fe powder (MP) were recorded under different environmental conditions, particularly at varying oxygen partial pressures. The corresponding peak intensities were plotted as a function of temperature. For each intensity plot, the composition of the surrounding atmosphere (N_2 + O_2) is indicated to reflect the oxygen availability during the oxidation process.

The results show that the extent of oxidation from metallic Fe to its oxide phases is directly influenced by the oxygen partial pressure. This is evident from the decreasing intensity of Peak 1 (P1), which corresponds to metallic Fe. A clear shift in the temperature associated with the onset of the oxidation reaction is also observed. As the oxygen partial pressure increases, the temperature at which the intensity of P1 begins to drop; shifts from approximately 755 °C to about 720 °C. This indicates that higher oxygen availability promotes oxidation at lower temperatures. Further the solid-solid phase transition can be seen using peak intensity P2 and P3 which are associated to two different oxide phases of iron.

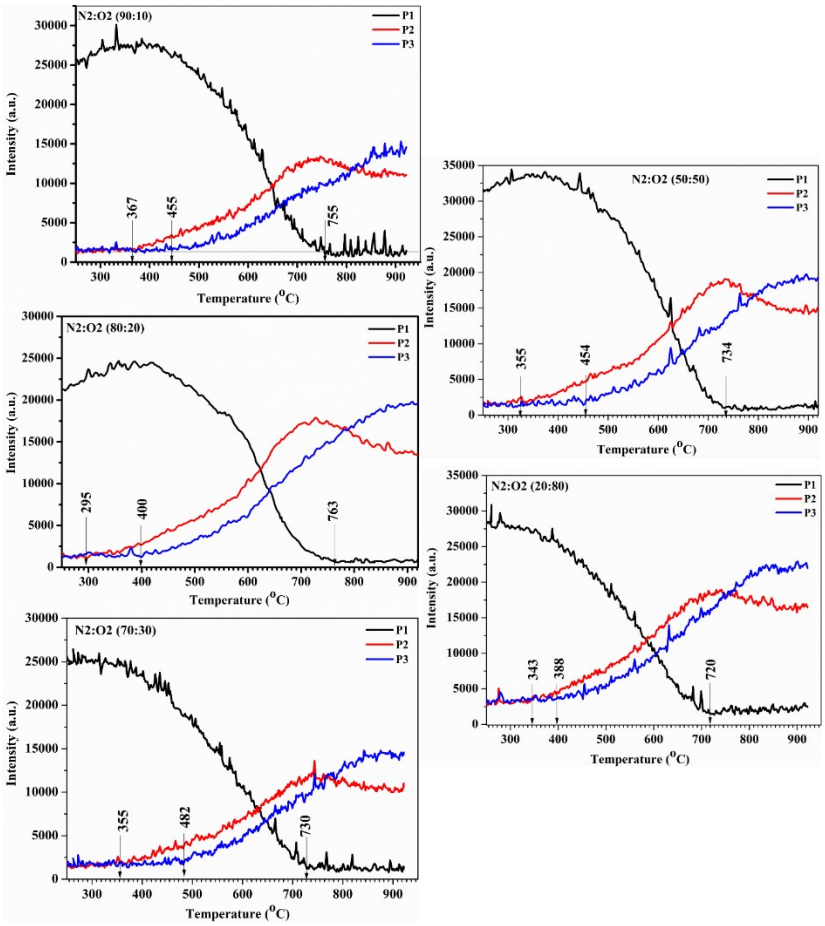

Figure S1*: shows the integrated intensities of three diffraction peaks recorded using in-situ XRD pattern as a function of temperature for M-Fe powder samples for different oxygen partial pressure values. Here, P1 corresponds to metallic Fe (JCPDF card no. # 851410), P2 to Fe_3O_4 / Y-Fe_2O_3 (JCPDF card no. #861362/ #391346), and P3 to α-Fe2O3 (JCPDF card no. 860550), representing the most intense (hkl) plane (110), (311), and (104), respectively.*

Maintaining moisture-free conditions, the initial and final temperatures corresponding to peaks P2 and P3 were plotted as a function of oxygen partial pressure, as shown in **Figure S2**. The black and blue temperature markers represent the onset of phase formation, whereas the red and pink markers correspond to the temperatures at which the respective phases reach their

maximum (saturation) intensities. For the first two oxygen partial pressures, the onset temperature of α-Fe_2O_3 extends up to the maximum temperature limit of 920 °C. Based on the data in **Figure S1**, it is still unclear whether this peak has fully saturated under these conditions. At higher oxygen partial pressures, the onset and maximum-intensity temperatures for each peak are clearly distinguishable. The information provided in **Figure S1** is therefore valuable for understanding the oxidation behavior at a given oxygen partial pressure under moisture-free conditions.

The rectangular frame at 20% oxygen highlights the onset temperatures for MF and MP under moisture-considered conditions. The influence of moisture on MP can be assessed by comparing the onset temperatures represented by solid rectangular markers (moisture-considered) with the corresponding moisture-free data points. When comparing the oxidation profiles, peak P2 is fully developed under moisture-considered conditions and exhibits a narrower temperature window relative to the moisture-free case. In contrast, the maximum intensity of P3 is not observed within the measured temperature range, suggesting that higher experimental temperatures may be required to stabilize the P3 phase. This comparison underscores the significant role of the processing environment - particularly moisture content - on the oxidation process. The hollow rectangular markers denote the onset temperature for MF under moisture-considered conditions.

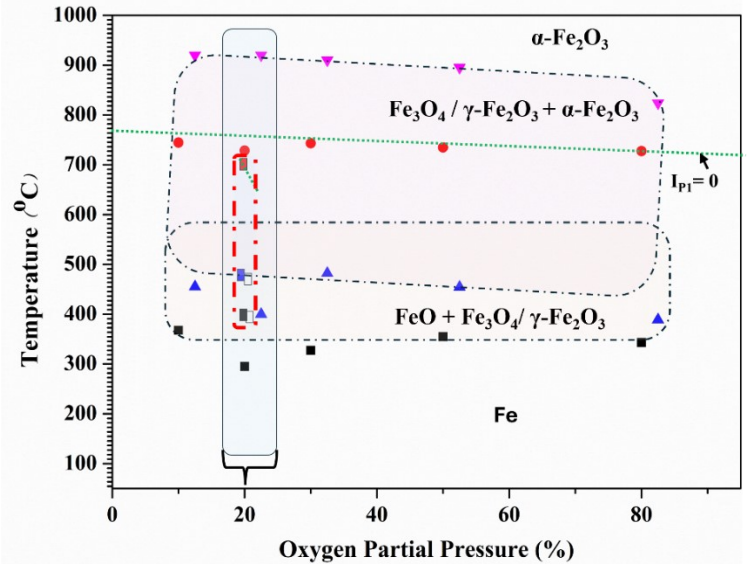

Figure S2: *In-situ XRD analysis of M–Fe powder recorded under different oxygen partial pressures to investigate phase evolution in a pure (moisture-free) environment. The initial and final temperatures (measured from* ***Figure S1****) are indicated by paired markers: black–red for P2 and blue–pink for P3. The green dotted line denotes the progressive decrease in P1 intensity, approaching zero with increasing oxygen partial pressure. An overlap of the results for MF-Air and MP-Air (Figure 5; moisture considered) is highlighted in the red dotted box, where solid rectangular markers correspond to the graph in Figure 5(b1) and hollow rectangular markers to Figure 5(a1), obtained at an oxygen partial pressure of 21% under a compressed airflow of 50 mL/min.*

The high-resolution spectra of MP and MP-Pure are presented in **Figure S3** for comparison. The surface chemical features of the bare MP particles are consistent with those of MP-Pure, exhibiting the characteristic broad $Fe2P_{3/2}$ and $Fe2P_{1/2}$ peaks at the corresponding lower and higher binding energies.

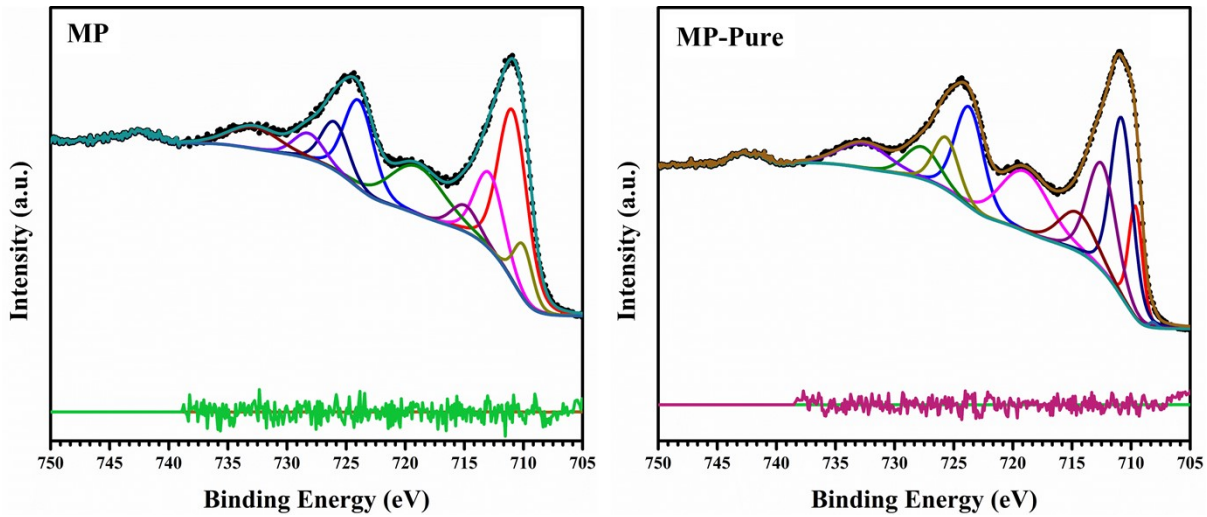

Figure S3: *High-resolution XPS Fe 2p spectra of the MP and MP-Pure sample.*

Scanning electron micrographs obtained under each processing condition are presented in **Figure S4** for direct comparison. In the OETO process, the presence or absence of a binder in the Fe system plays a dominant role in determining the resulting morphology, whereas the heating rate shows comparatively minimal influence. In contrast, the CETO process, characterized by a rapid heating rate of 12 °C/s; highlights the strong influence of oxygen partial pressure on surface morphology. Overall, these observations demonstrate that by understanding the individual effects of processing parameters, tailored surface morphologies can be achieved in iron-oxide–based systems.

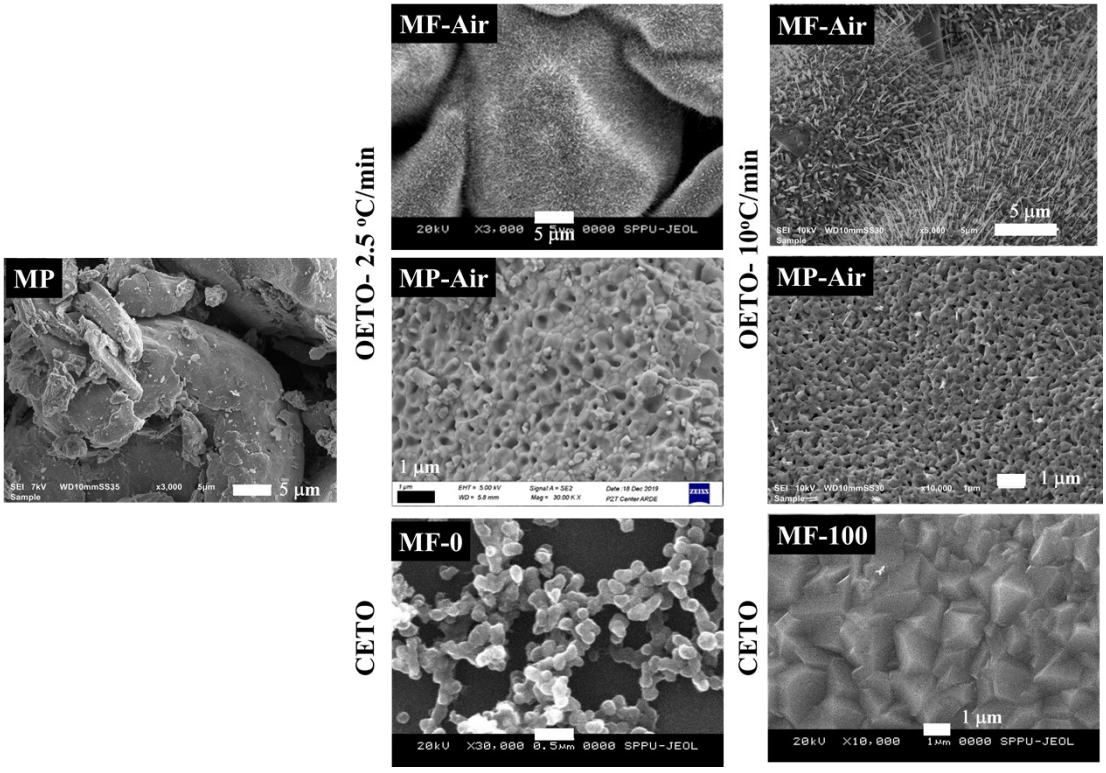

Figure S4*: Scanning electron micrographs illustrating the morphological changes of the sample surfaces pre- and post-processing, obtained under the experimental conditions specified in Table 2.*